Supplementary Material

for

Perfluorohexyloctane (F_6H_8) as a delivery agent for cyclosporine A in dry eye syndrome therapy – Langmuir monolayer study complemented with infrared nanospectroscopy

Anna Chachaj-Brekiesz[a*)], *Anita Wnętrzak*[a], *Ewelina Lipiec*[b,c], *Jan Kobierski*[d], *Patrycja Dynarowicz-Łątka*[a]

[a] Faculty of Chemistry, Jagiellonian University, Gronostajowa 2, 30-387 Kraków, Poland

[b] Faculty of Physics, Astronomy and Applied Computer Science, Jagiellonian University, Łojasiewicza 11, 30-348 Kraków, Poland

[c] The Henryk Niewodniczański Institute of Nuclear Physics, Polish Academy of Sciences, Radzikowskiego 152, 31-342 Kraków, Poland

[d] Department of Pharmaceutical Biophysics, Faculty of Pharmacy, Jagiellonian University Medical College, Medyczna 9, 30-688 Kraków, Poland

*) Corresponding author e-mail: chachaj@chemia.uj.edu.pl

Table of contents:

1. Experimental section

1.1. Materials

DPPC (1,2-dipalmitoyl-sn-glycero-3-phosphocholine), DPPE (1,2-dipalmitoyl-sn-glycero-3-phosphoethanolamine) and egg SM (containing 86% of N-(hexadecanoyl)-sphing-4-enine-1-phosphocholine) of >99% purity were obtained from Avanti Polar Lipids; CsA (Cyclosporin A) was purchased from Sigma-Aldrich; F_6H_8 (perfluorohexyloctane) was delivered from Novaliq GmbH. Spectral-grade chloroform (stabilized with ethanol) and ethanol were supplied by Sigma-Aldrich. All chemicals were used without further purification. Stock chloroform solutions of the investigated compounds were prepared with a typical concentration of 0.2–0.3 mg mL^{-1}. Then, appropriate volumes of basic solutions were mixed to obtain aliquots for Langmuir and Langmuir-Blodgett studies. Deionized ultrapure water from a Milipore system with a resistivity of 18.2 MΩ·cm was used as a subphase. For AFM experiments, ruby muscovite mica sheets of quality grade V1 (Continental Trade) were used as solid supports. Before LB transfer, the mica surface was cleaned by cleavage with an adhesive tape. For AFM-IR experiments, wafers coated with gold were prepared basing on the published procedure [1].

1.2. Methods

1.2.1. Langmuir and Langmuir-Blodgett monolayer technique

The surface pressure-area isotherms (π-A) were obtained with NIMA 301S trough, with a total area of 300 cm^2, thermostated by circulating water (20 °C ± 0.1 °C). Single Teflon barrier was applied to compress monolayers with constant speed set as 20 cm^2/min. The surface pressure was continuously monitored during film compression by the Wilhelmy plate method with a sensitivity of ± 0.1 mN/m. Langmuir monolayers were prepared by spreading a known amount of appropriate solutions on a water subphase with a microliter syringe and 10 min was allowed to elapse for complete solvent evaporation before starting the measurements. Each measurement was repeated 2–3 times to ensure high reproducibility of the obtained isotherms to ± 1-2 $Å^2$/molecule.

The transfer of selected Langmuir monolayers onto solid substrate (mica or silica wafers coated with gold) was carried out using NIMA 612D (total area = 600 cm^2). In order to perform the LB transfer, the solid substrate was placed in the subphase. Then, the film was spread and compressed to the surface pressure of 15 mN/m (the highest surface pressure at which the investigated monolayers were found to be stable). After monolayer stabilization (≈ 10-15 min), the film was transferred onto substrate using a dipper speed of 3 mm min^{-1}. Deposition

conditions were selected based on preliminary experiments, including: analysis of π-A isotherms and BAM images, stability experiments as well as screening studies using AFM. In each transfer experiment, single layer was deposited and the transfer ratio values were close to 1.

1.2.2. Brewster angle microscopy (BAM)

Texture of floating monolayers was directly observed with ultraBAM instrument (Accurion GmbH). The application of 50-mW laser emitting *p*-polarized light at a wavelength of 658 nm, a 10x magnitude objective, a polarizer, an analyzer, and a CCD camera allowed a spatial resolution of 2 μm. The angle of observation was set as 53.1°, polarization at 2°, and analyzer at 10°. Brewster angle microscope was installed over a double-barrier Langmuir trough (KSV, total area = 700 cm^2). The procedure of monolayers formation was identical to that described in previous section. BAM images presented in this paper show monolayer fragments of 720 μm × 400 μm.

1.2.3. AFM imaging

An acquisition of AFM topographies was performed in ambient with NT-MDT instrument (Zelenograd, Russia) in non-contact mode. Areas of 1 μm × 1 μm − 10 μm × 10 μm were scanned. The used imaging speed was low (scan rate 0.2–0.5 Hz). Commercially available NSG01 cantilevers (resonant frequency: 87 kHz–230 kHz, force constant 1.45 N/m–15.1 N/m, tip curvature radius: 6 nm–10 nm, purchased by NT-MDT) were used for AFM imaging. Gwyddion (ver. 2.30) software was applied for obtained data processing. Acquired images were flattened (2-nd order polynomial).

1.2.4. AFM-IR

AFM-IR data was acquired using nanoIR2 instrument (Anasys, Santa Barbara, CA, USA), equipped with a commercially available tunable infrared quantum cascade laser, QCL (Daylight Solutions MIRcat). The laser covered whole fingerprint spectral region with three stages: 1929–1695 cm^{-1}, 1695–1410 cm^{-1}1 and 1410–1145 cm^{-1}. AFM-IR spectra were collected in contact mode. Silicon gold coated probes PR-EXnIR2-10 (20 nm tip apex diameter, res. freq. 13 ± 4 kHz, spring. const. 0.07–0.4 N/m) manufactured by Anasys Instruments were applied. Two perpendicular polarizations of infrared laser light were applied in order to probe functional groups oriented perpendicular and parallel to the substrate surface. Single IR absorption spectra were in the spectral range of 1929–1145 cm^{-1} with 256 scans co–added. The spectral resolution

was 2 cm^{-1}. Spectra were processed in OPUS software. Smoothing was applied (Savitzky-Golay method, number of smoothing points: 9–13). In order to visualize and compare spectral shape/peak ratios of ATR-FTIR, AFM-IR (p-polarization) and AFM-IR (s-polarization), the acquired spectra were normalized (vector normalization algorithm).

1.2.5. IR spectroscopy

ATR-FTIR (Attenuated Total Reflection Fourier Transform Infrared) spectra (in the range of 4000 cm^{-1}–600 cm^{-1}) of were acquired with a Nicolet Almega microscope system equipped with a single bounce diamond Micro–ATR with the diamond top plate option. Spectra were collected with a spectral resolution of 4 cm^{-1} 64 scans were co–added for each spectrum. Obtained ATR–FTIR data was processed in Opus 6.5 software. Extended ATR correction (number of ATR reflections: 1; ATR angle of incidence: 45; mean refraction index of the sample: 1.5) was used. Each spectrum was also smoothed (using Savitzky-Golay method, number of smoothing points: 5) and then baseline of each spectrum was corrected (rubber–band correction with 16 baseline points and 2–4 iterations).

1.2.6. Theoretical calculations

The initial structure of CsA was taken from the Protein Data Bank [2,3]. Geometry optimization and frequency calculation for CsA, DPPE, DPPC, SM, and F_6H_8 were performed using Density Functional Theory (DFT) modeling through the GAUSSIAN 16 software package [4]. The frequency calculations were based on priorly optimized structures. All calculations were performed using the B3LYP functional [5–8] with 6-31g(d) basis set. Systems have been optimized using the default UltraFine integration grid, default integer values and a combination of EDIIS and CDIIS tight convergence procedures, with no damping or Fermi broadening.

The DFT methods overestimate the vibrational frequencies. It is caused by anharmonic effects and approximation of electronic structure, i.e. incomplete inclusion of electron correlations and the use of finite basic set. To avoid this factor, the raw frequencies obtained from the vibrational simulation were scaled by 0.96 [9]. DFT optimized geometries were visualized in Gabedit software [10].

2. Supplementary figures

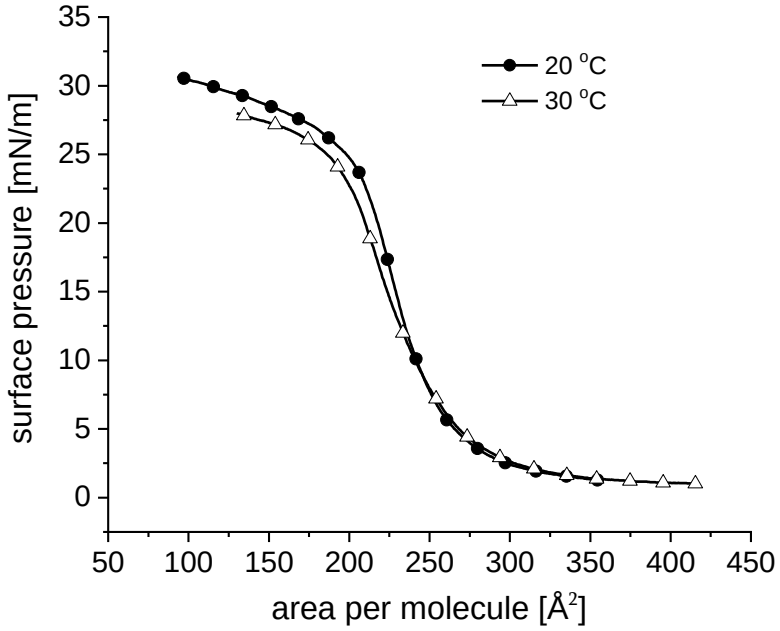

Figure S.1. π–A isotherms of CsA registered for different subphase temperatures.

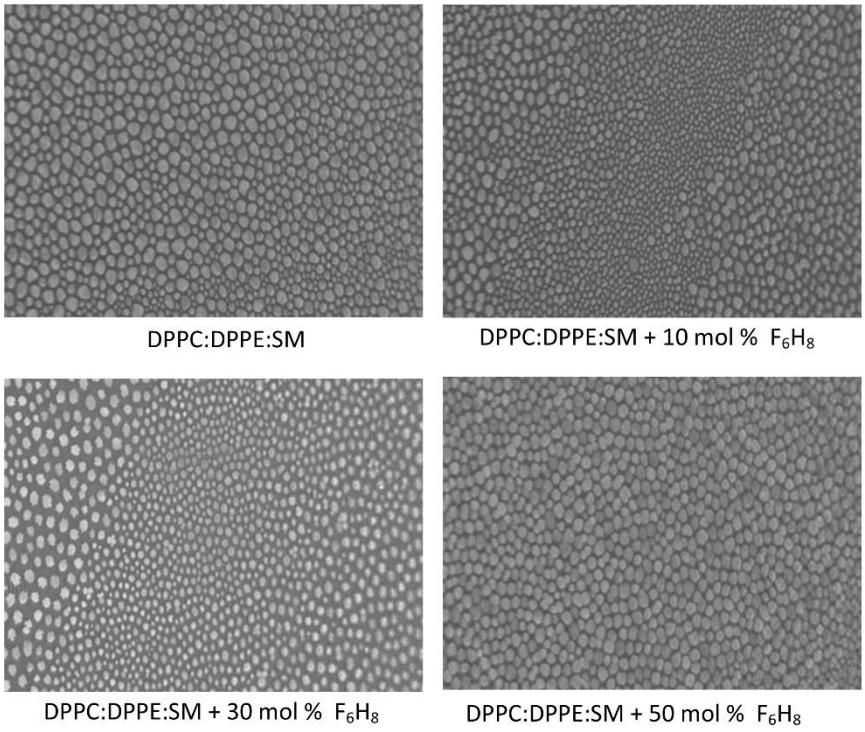

Figure S.2. BAM images of DPPC:DPPE:SM monolayer with and without F_6H_8 at 15 mN/m (each image shows monolayer fragments of 720 μm x 400 μm).

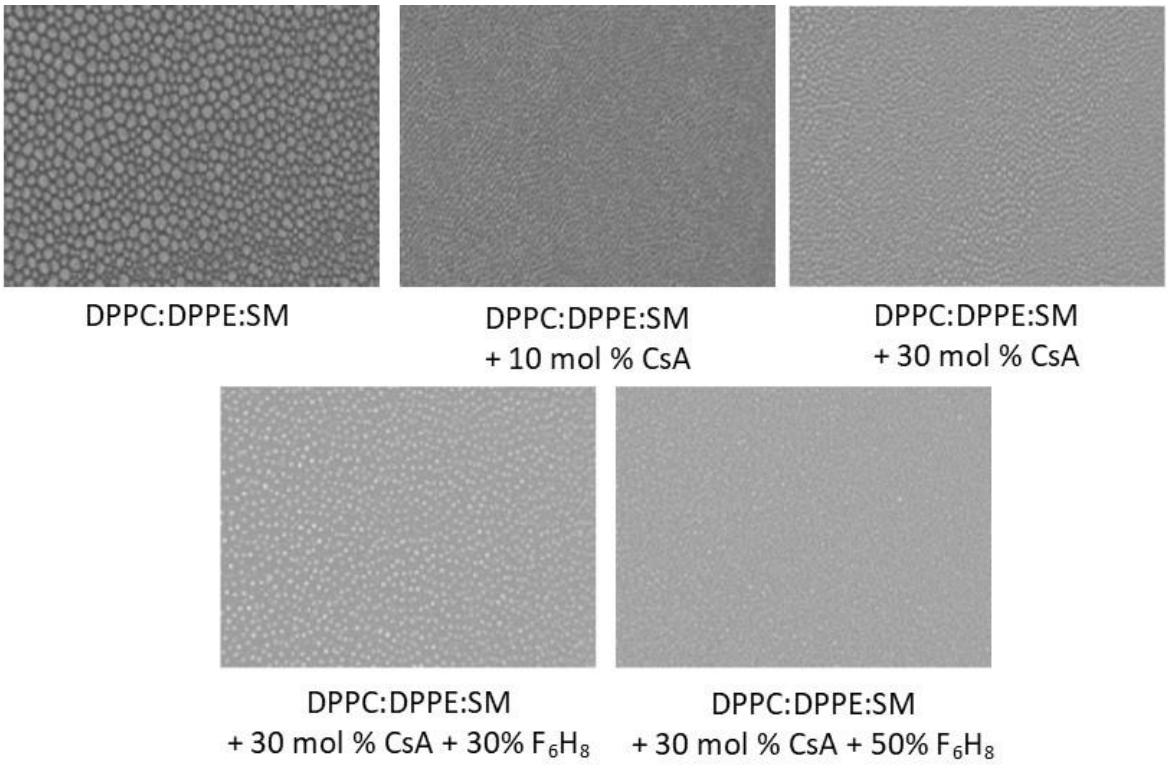

Figure S.3. BAM images at 15 mN/m for pure DPPC:DPPE:SM monolayer; systems treated with different amounts of CsA with and without addition of F_6H_8 (each image shows monolayer fragments of 720 μm x 400 μm).

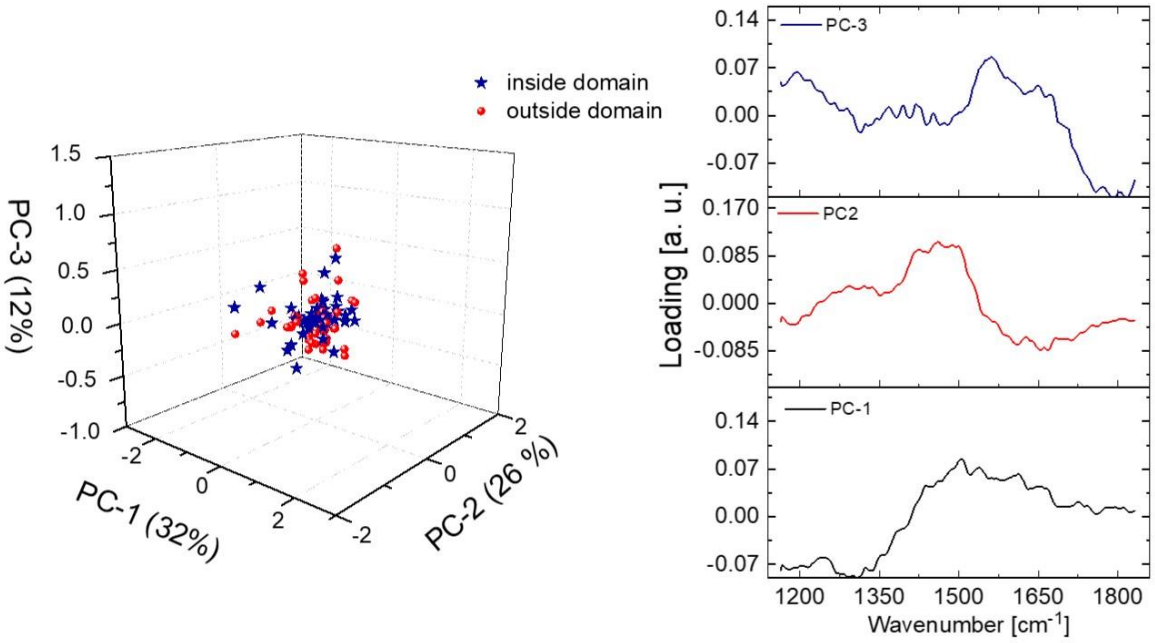

Figure S.4. PCA analysis of AFM-IR spectra collected with s-polarised light from the domains and from the neighbouring areas.

3. Theoretical and experimental IR spectra of the investigated pure compounds

As a part of initial studies, experimental infrared spectra of bulk samples (phospholipids (DPPC, DPPE, SM) and pharmaceuticals (CsA and F_6H_8)) were compared to those calculated by DFT approach with B3lYP method and 6-31g(d) basis set (Fig. S.5 in Appendix A). Assignments of selected bands (both calculated and recorded) were collected in Table S.1. A good agreement between measured and theoretical spectra can be seen for each system component. For the CsA molecule, broad band 1450-1550 cm^{-1} was attributed to bending of N-H with stretching of C-N, while intensive band 1600-1700 cm^{-1} is mostly due to stretching modes of C=O [11]. This is confirmed by our simulation. Moreover, strong peaks at 1368 cm^{-1}, 1386 cm^{-1}, and 1409 cm^{-1} are caused by the stretching of C-N and bending in CH_3 groups of VAL, MVA, MLE, BMT and ABA (for details, see Appendices B-F).

IR bands observed for SM at 1545 cm^{-1} and 1640 cm^{-1}, assigned to the C=O and N–H vibrations in amide group [12] in the calculated spectrum, are shifted into 1701 cm^{-1}. The broad experimental band at 1200-1250 cm^{-1}, attributed to asymmetric stretch vibrations of phosphodioxy groups [12] (1250 cm^{-1} in the calculation) additionally consists of C-N stretching and bending of C-H in choline. Bending C-H vibrations in the acyl and alkyl chain are responsible for bands near 1480 cm^{-1} and 1375 cm^{-1} [13], which was confirmed in our calculations.

In DPPC and DPPE molecules bands near 1470 cm^{-1} were assigned to scissoring modes of CH_2 group, while stretching of C=O was responsible of bands near 1740 cm^{-1}, which is consistent with previous reports [14]. Additional band near 1250 cm^{-1} caused by stretching of P=O was observed.

Table S.1. Vibrational assignments of observed and calculated frequencies for investigated compounds in the spectral range 1150-1900 cm^{-1}. ν – stretching, δ – scissoring, ω – wagging, ρ – rocking, τ – twisting. **ABA**, aminobutyric acid; **BMT**, butenylmethylthreonine; **CsA**, cyclosporine A; **DAL,** D-alanine; **DPPC**, 1,2-dipalmitoyl-sn-glycero-3-phosphocholine; **DPPE**, 1,2-dipalmitoyl-sn-glycero-3-phosphoethanolamine; **F_6H_8**, perfluorohexyloctane; **MLE**, methylleucine; **MVA**, methylvaline; **SAR**, sarcosine; **SM,** sphingomyelin; **VAL**, valine.

Compound	Wavenumber observed in ATR-FTIR (cm^{-1})	Wavenumber calculated (cm^{-1})	Assignments
CsA	1600-1700	1702.19	ν(C=O) in BMT
		1693.49	ν(C=O) in ALA and MLE
		1678.97	
		1667.40	ν(C=O) in MLE
		1658.96	
		1651.28	ν(C=O) in DAL
		1646.46	ν(C=O) in VAL and MLE
		1639.43	ν(C=O) in MVA
	1450-1550	1509.82	ν_{as}(C-N), δ(C-N), δ(C-H)
		1499.95	
		1484.54	
		1479.56	
		1472.38	
		1463.18	
		1451.09	
	1350-1450	1403.25	ν(C-N) in MLE δ(C-H) in CH_3 in VAL
		1398.68	δ(C-H) in CH_3 in MLE
		1393.35	ν(C-N) in SAR δ(C-H) in CH_3 in MVA
		1385.00	δ(C-H) in CH_3 in ABA
		1382.93	δ(C-H) in CH_3 in BMT
SM	1545, 1640, 1656	1700.95	ν(C=O), δ(C-N) in amide group
	-	1667.97	ν(C=C)
	1487	1440.57	δ(O-H)
	1466	1479.94	ν(C-N), ν(N-H)
	1437	1440.57	ν(O-H)
	1378	1368.31	ν_{as}(C-C), ω(C-H)
	1200-1250	1210.13	δ(C-H), τ(C-H), ω(C-H) in choline
		1225.25	ν(C-N), τ(C-H)
		1250.64	ν_{as}(P=O)
F_6H_8	1234	1219.43	ν(C-F), ν(C-C), ω(C-H)
	1188	1180.02	ν(C-F), ν(C-C), ρ(C-H), τ(C-H)
	1143	1136.79	ν(C-F), ν(C-C), ω(C-H)
DPPC	1745	1745.10	ν(C=O)
	1726	1730.18	
	1507	1497.41	δ(C-H) in choline
	1470	1475.10	δ(C-H)
	1260	1252.04	ν(P=O), ν(C-N), ρ(C-H)
	1172	1182.06	ν(C-O), τ(C-H)
	1160	1162.59	
DPPE	1741	1748.34	ν(C=O)
	1440-1475	1470.95	δ(C-H)
		1462.32	
	1243	1251.45	ν(P=O), ω(C-H)
	1223	1214.66	ν(C-O), τ(C-H)
	1178	1154.13	
	1145	1146.62	ν(P=O), ρ(O-H), ω(C-H)

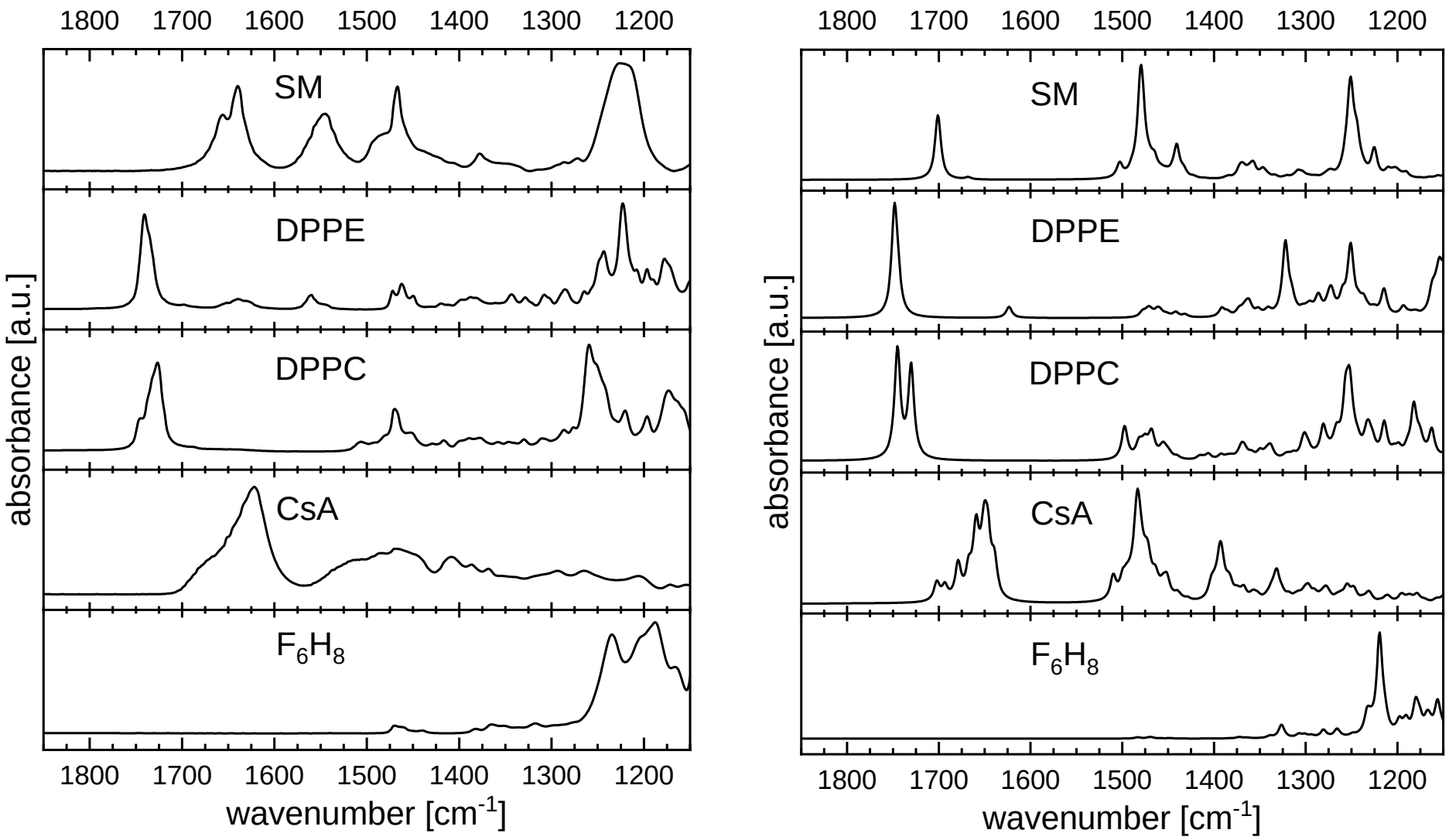

Figure S.5. ATR-FTIR spectra (left panel) and calculated IR spectra (right panel) of studied compounds

4. References

[1] L.T. Banner, A. Richter, E. Pinkhassik, Pinhole-free large-grained atomically smooth Au(111) substrates prepared by flame-annealed template stripping, Surf. Interface Anal. 41 (2009) 49–55. doi:10.1002/sia.2977.

[2] Protein Data Bank: 1CYA, (n.d.). doi:10.2210/pdb1CYA/pdb.

[3] S.W. Fesik, R.T. Gampe, H.L. Eaton, G. Gemmecker, E.T. Olejniczak, P. Neri, T.F. Holzman, D.A. Egan, R. Edalji, R. Simmer, NMR studies of [U-13C]cyclosporin A bound to cyclophilin: bound conformation and portions of cyclosporin involved in binding., Biochemistry. 30 (1991) 6574–83.

[4] D.J. Frisch, M. J.; Trucks, G. W.; Schlegel, H. B.; Scuseria, G. E.; Robb, M. A.; Cheeseman, J. R.; Scalmani, G.; Barone, V.; Petersson, G. A.; Nakatsuji, H.; Li, X.; Caricato, M.; Marenich, A. V.; Bloino, J.; Janesko, B. G.; Gomperts, R.; Mennucci, B.; Hratch, Gaussian 16, Revision B.01, (2016).

[5] A.D. Becke, Density-functional thermochemistry. III. The role of exact exchange, J. Chem. Phys. 98 (1993) 5648–5652. doi:10.1063/1.464913.

[6] C. Lee, W. Yang, R.G. Parr, Development of the Colle-Salvetti correlation-energy formula into a functional of the electron density, Phys. Rev. B. 37 (1988) 785–789. doi:10.1103/PhysRevB.37.785.

[7] S.H. Vosko, L. Wilk, M. Nusair, Accurate spin-dependent electron liquid correlation energies for local spin density calculations: a critical analysis, Can. J. Phys. 58 (1980) 1200–1211. doi:10.1139/p80-159.

[8] P.J. Stephens, F.J. Devlin, C.F. Chabalowski, M.J. Frisch, Ab Initio Calculation of Vibrational Absorption and Circular Dichroism Spectra Using Density Functional Force Fields, J. Phys. Chem. 98 (1994) 11623–11627. doi:10.1021/j100096a001.

[9] Precomputed vibrational scaling factors, (n.d.).

[10] A.-R. Allouche, Gabedit-A graphical user interface for computational chemistry softwares, J. Comput. Chem. 32 (2011) 174–182. doi:10.1002/jcc.21600.

[11] Z. Qu, H. Zhu, V. May, Unambiguous Assignment of Vibrational Spectra of Cyclosporins A and H †, J. Phys. Chem. A. 114 (2010) 9768–9773. doi:10.1021/jp102206z.

[12] I. Dreissig, S. Machill, R. Salzer, C. Krafft, Quantification of brain lipids by FTIR spectroscopy and partial least squares regression, Spectrochim. Acta Part A Mol. Biomol. Spectrosc. 71 (2009) 2069–2075. doi:10.1016/J.SAA.2008.08.008.

[13] C. Krafft, L. Neudert, T. Simat, R. Salzer, Near infrared Raman spectra of human brain lipids, Spectrochim. Acta Part A Mol. Biomol. Spectrosc. 61 (2005) 1529–1535. doi:10.1016/J.SAA.2004.11.017.

[14] A. Blume, Properties of lipid vesicles: FT-IR spectroscopy and fluorescence probe studies, Curr. Opin. Colloid Interface Sci. 1 (1996) 64–77. doi:10.1016/S1359-0294(96)80046-X.